

Supporting Information

Kim et al. 10.1073/pnas.0807935105

SI Text

Cultivation of Microorganisms and Culture Media. Bacterial species of *Azotobacter vinelandii* (Av, ATCC 12837), *Bacillus licheniformis* (Bl, ATCC 25972), and *Paenibacillus curdlanolyticus* (Pc, ATCC 51899) were purchased from the American Type Culture Collection. Av cells were enriched in sterilized *Azotobacter* 1771 medium (ATCC; 10.0 g/L D-(+)-glucose, 1.2 g/L CH₃COONH₄, 0.583 g/L K₂HPO₄, 0.224 g/L KH₂PO₄, 0.1 g/L CaSO₄·2H₂O, 0.098 g/L MgSO₄, 0.058 g/L NaCl, 0.005 g/L FeSO₄·7H₂O, and 0.0002 g/L Na₂MoO₄·2H₂O, pH 6.8). Both Bl and Pc cells were enriched in 30 g/L of sterilized trypticase soy broth (TSB) medium (BD Company). During the cultivation of Pc species, cellulolytic enzymes were induced by adding filter-sterilized (0.45 μm, Whatman) carboxymethyl-cellulose (CM-cellulose; sodium salt, 0.7 degree of substitution, Sigma-Aldrich) at 1 g/L final concentration. Seed cultures of each species were cultured in a rotary shaking incubator (SI-600 Lab Companion, Jeio Tech) at 30°C and 180 rpm in a Laurell Model WS-400A-GNPP/LITE rotor. Species were subcultured every 3 days on fresh agar medium and were preserved at 4°C by using 40 g/L of sterilized Difco tryptic soy agar (TSA) medium (BD Company) for Bl and Pc species and 1771 agar medium containing 2% (wt/vol) agar (Fisher Scientific) for Av species. The minimal buffer was composed of 0.5 g/L KH₂PO₄, 0.2 g/L K₂HPO₄, 0.1 g/L NaCl, 0.1 g/L MgSO₄·7H₂O, 0.05 g/L FeSO₄·7H₂O, and 0.001 g/L Na₂MoO₄·2H₂O (pH 6.9). The cellulose/penicillin (CP) medium consisted of carboxymethyl cellulose (1 g/L) and penicillin G (100 mg/L) in minimal buffer solution.

In Fig. 1B, mixed culture was performed in a test tube (14 ml, Falcon) containing 2 ml of either nutrient-rich medium (TSB/1771 mixture, 4:1, vol/vol) or nutrient-poor medium (CP medium including 100 μg/L D-glucose) at 30°C and 160 rpm for 36 h. Live-cell numbers of Av, Bl, and Pc were adjusted to similar levels via live/dead staining and cell counting (Live/Dead BacLight Bacterial Viability kit, Molecular Probes) before inoculation. The number of viable cells in macroscale cultures was estimated by agar plate counting. We confirmed that all three species grew on both TSB and 1771 agar media (data not shown). Differences in colony morphology on the agar plate enabled differentiation and simultaneous counting of cell numbers.

Inoculation and Cultivation of Species in the Microfluidic Device.

After seed cultures of Av, Bl, and Pc species at exponential phase were harvested and washed twice with minimal buffer solution, the live-cell number of each species was adjusted to a similar level by staining with live/dead dye and counting cells under an epi-fluorescence microscope (DMI 6000 B, Leica), resulting in a live-cell density of $\approx 10^6$ CFU/ml. The cell suspension of each species was transferred aseptically to sterilized Gastight syringes (1805 RN, Hamilton) with 30-gauge Teflon tubing (Weico) sealed to Teflon tubing (i.d./o.d. = 100/150 μm, polytetrafluoroethylene [PTFE], Zeus) with wax. The cell suspension in the syringes was inoculated accurately into an individual culture well in the microfluidic device at a density of ~ 500 –1000 live cells/well via a microaspirator (Stoelting) under a stereomicroscope (SMZ-2E, Nikon). The number of live cells loaded into each well varied by $\pm 10\%$. The inoculated device was placed over a droplet of appropriate medium on a siliconized glass cover slide, and the medium filled the communication channel below the wells. The device setup was fixed inside the Petri dish using silicone vacuum grease (Dow Corning), and the Petri dish containing the device setup then was incubated in an inverted

position at 30°C. Water droplets were added on the bottom of the inside of a Petri dish to maintain humidity. Three replicates of the microfluidic devices were performed at each time point for the experiments shown in Figs. 2 and 3. The low-nutrient/antibiotic medium (CP medium) contained carboxymethyl cellulose (1 g/L) as a sole carbon source, no nitrogen source, and penicillin G (100 mg/L). The nutrient-rich medium was a mixture of TSB and 1771 media in a 4:1 (vol/vol) ratio. The number of live cells in a microfluidic device was counted manually after the live/dead staining with solutions of SYTO9 (live, green) and propidium iodide (dead, red) (Molecular Probes).

Data Acquisition and Analysis of Microscopic Images. Bacterial species of Av, Bl, and Pc were stained with a fluorescent dye (Molecular Probes) to indicate live (green; SYTO9) and dead (red; propidium iodide) cells. After loading the live/dead dye into culture wells using the microaspirator (Stoelting), a cover glass (48 × 65 mm, Gold Seal, Thermo Scientific) was placed over the culture wells, and the microfluidic device was inverted to take images. Cells were imaged using an epi-fluorescence microscope (DMI 6000 B, Leica) equipped with a 5× (0.15 N.A.) or a 20× (0.40 N.A.) objective and either an L5 or a TX2 filter set (Leica), which were coupled with a cooled CCD camera (12-bit, 1344 × 1024 resolution; Hamamatsu Photonics) with a 1.0× coupler.

The exposure time of fluorescent images in Figs. 2 and 3 was 100 ms. Among the three replicates of microfluidic devices, images from one of the devices were selected randomly as the representative setup of fluorescent images. In Fig. 2A (Top), the fluorescent images taken with both filters at 0 h were processed with the low scale value of 250 and the high scale value of 3000 (e.g., L250 H3000) for Av, L250 H3000 for Bl, and L250 H1000 for Pc. In Fig. 2A (Bottom), the fluorescent images of the connected community, taken at 36 h, were processed with scales of L250 H800 for Av, 250 H800 for Bl, and L250 H600 for Pc. In Fig. 2B, the fluorescent images of isolated species, taken at 36 h, were processed with scales of L250 H800 for Av, L250 H800 for Bl, and L220 H400 for Pc. In Fig. 3A, the fluorescent images of the mixed culture taken with both filters were processed with scales of L250 H3000 at 0 h and L250 H800 at 36 h, respectively. Images taken with both filters, L5 and TX2, were overlaid using MetaMorph image software (Molecular Devices). The intensity profile of fluorescent images in Figs. 2 and 3 is provided in Fig. S9. The number of live cells in an overlaid fluorescent image was counted manually in a digitally enlarged image. Replicate counts of the same image showed variations within 3%. For the graphs in Figs. 2 and 3, at least three replicates of each device were counted and quantified. To quantify live cells in a mixed culture in Fig. 3, the total number of live cells was estimated without discrimination of species.

Survival Ratio of Av, Bl, and Pc Species. In Fig. S1A, the survival ratio of each species was calculated from the number of viable cells in different media conditions over time. After each species was enriched in liquid cultures of either TSB medium (for Bl and Pc) or 1771 medium (for Av), cells were washed twice with minimal buffer solution, then adjusted to have a similar cell density of $\approx 10^7$ CFU/ml. For the culture, three different media were prepared; no-nutrient (minimal buffer solution; see Cultivation of Microorganisms and Culture Media), low-nutrient (minimal buffer solution supplemented with 500 μM glucose and 500 μM ammonium phosphate), and no-nutrient with antibiotics

(minimal buffer solution with 100 mg/L penicillin G). After cells were inoculated onto each medium, cultures were carried out at 30°C, 150 rpm, for 36 h. The number of viable cells was estimated by using the agar plate counting of cfus.

Measurement of Specific Growth Rate in Monoculture of Av and Bl. In Fig. S1B, cultivation of individual species of Av or Bl was performed in 14-ml test tubes (Falcon, Becton Dickinson Labware) with a 3-ml working volume of medium at 30°C and 180 rpm in a rotary shaker for 3 h. Media with different concentrations were prepared by the serial dilution of a mixture of TSB and 1771 media (4:1, vol/vol). The initial concentration of the mixture TSB/1771 medium was 30 g/L; it then was diluted to various concentrations: 0.05, 0.1, 0.3, 0.6, 1.0, 10, and 50 mg/L. During the cultivation, aliquots of culture broth of both Av and Bl were taken intermittently and used for measuring optical density at 600 nm (8453 UV-Visible Spectrophotometer, Agilent Technologies). The dry cell weight of both Av and Bl species was obtained from the respective calibration curve of optical density units versus the dry cell weight of each species. The specific growth rate (μ) of both Av and Bl cells was calculated by the equation $\mu = 1/X(dX/dt)$, where μ is the specific growth rate (h^{-1}), X is the dry cell weight (g/L), and t is the cultivation time.

Effect of Heat-Killed Bl Cell Debris on the Viability of Av and Pc Cells. Fig. S1C shows the results of an experiment to test the effect of cell debris of the Bl species on the viability of cells of either the Av or Pc species. Heat-killed Bl cell debris was prepared by taking a Bl cell suspension, enriched in TSB medium and with a cell density of $\approx 10^6$ CFU/ml, washing the suspension in minimal buffer, and then autoclaving the suspension at 121°C for 15 min. After Av and Pc cells were enriched, washed twice, and re-suspended in CP medium supplemented with 100 $\mu\text{g/L}$ glucose at $\approx 10^5$ CFU/ml, the heat-killed Bl cell suspension (0.1 ml) was added to either the Av or Pc cell suspension (0.9 ml), and the resulting suspension was incubated at 30°C, 150 rpm, for 36 h. Samples from the Av or Pc cultures were harvested intermittently and used for the viable cell counting.

Effect of Penicillin and Its Degradation Products on the Viability of Av and Pc Cells. Fig. S1D shows the results of an experiment to test the effect of degradation products of penicillin G on the viability of Av and Pc cells. Each species was cultured in four different media: the control medium (minimal buffer containing 1 g/L CM-cellulose and 100 $\mu\text{g/L}$ glucose), the control medium containing 100 mg/L penicillin G (w/PEN), the control medium containing degradation products of penicillin G (w/PEN degradants), and the control medium containing 0.5 mg/L β -lactamase (w/ β -Lactamase). To obtain the degradation products of penicillin G, 0.5 mg/L β -lactamase (Penicillinase from *Bacillus cereus*, Sigma) was incubated in the minimal buffer containing 100 mg/L penicillin G (Fisher Scientific) for 1.5 h at room temperature. Thin-layer chromatography (TLC) was performed to monitor qualitatively the conversion of penicillin G into its degradation products. Silica gel TLC plates (PE SIL G/UV, 250- μm layer, polyester, Whatman) with sample spottings were eluted with mobile phase of ethyl acetate: acetone: water (1:2:1, vol/vol/vol), then developed by using iodine. It was confirmed that the commercial β -lactamase fully degraded the penicillin G in ≈ 3 min. The degradation products were added to cultures of either Pc or Av and incubated at 30°C, 160 rpm. Aliquots were taken intermittently and used for monitoring the number of viable cells by plate counting in TSA (for Pc) or 1771 agar media (for Av).

Confirmation of Localized Growth of Bacterial Species in the Microfluidic Culture Well. In Fig. S2, the fluorescence-labeled bacterial strains used were (i) GFP-labeled *Escherichia coli* containing

PUCP24/EGFP plasmids in *E. coli* K12 YMel-1 host and (ii) RFP-labeled *E. coli* containing DsRed-encoding plasmids in *E. coli* DH10B host. The RFP-labeled *E. coli* strain was provided by Professor Benjamin Glick of the University of Chicago. GFP-labeled *E. coli* was cultured in TSA medium (BD Company) that included 100 mg/L kanamycin and 20 mg/L gentamicin. RFP-labeled *E. coli* was cultured in TSA medium that included 100 mg/L ampicillin. After both strains were suspended in the saline solution (0.9% of sterilized NaCl solution, wt/vol), the numbers of fluorescent cells of each strain were adjusted by dilution to be similar using an epi-fluorescence microscope (DMI 6000 B, Leica). Then, each strain was transferred into a glass syringe and was inoculated accurately into a separate, individual culture well of a microfluidic device by using a microaspirator (Stoelting) under a stereomicroscope (SMZ-2E, Nikon). One of the three culture wells was loaded with GFP-labeled *E. coli*, one of the culture wells was loaded with RFP-labeled *E. coli*, and one of the culture wells was left vacant. Three replicates of the microfluidic devices were performed in the experiment for each time point. After the wells were loaded, the microfluidic device was placed on the surface of a siliconized glass cover slide (22 \times 22 mm, Hampton Research), and the communication channel was filled with TSB medium (BD Diagnostics) without any antibiotic pressure. The inoculated microfluidic device setup was fixed inside a Petri dish by using silicone vacuum grease (Dow Corning); then the Petri dish containing the device setup was incubated in an inverted position at 30°C for 12 h. Water droplets were added on the bottom of the inside of the Petri dish to maintain humidity.

For the fluorescent images at 0 h in Fig. S2B, images of the GFP-labeled *E. coli* strain and the RFP-labeled *E. coli* strain were taken by an epi-fluorescence microscope equipped with a 20 \times objective (0.40 N.A.) and an L5 filter (for the GFP-labeled *E. coli* strain) or a TX2 filter (for the RFP-labeled *E. coli* strain) at 150 ms exposure time. After fluorescent images were processed at the low scale value of 200 and the high scale value of 270, a rectangle shape was collected from the center of a culture well inoculated with either the GFP-labeled *E. coli* strain or the RFP-labeled *E. coli* strain. For the fluorescent images at 12 h in Fig. S2B, images of the GFP-labeled *E. coli* strain and the RFP-labeled *E. coli* strain were taken by an epi-fluorescence microscope equipped with a 5 \times objective (0.15 N.A.) and an L5 filter (for GFP-labeled *E. coli*) or a TX2 filter (for RFP-labeled *E. coli*) at 10 ms of exposure time. The reproducibility among three replicates of microfluidic devices was confirmed in all cases, and one of the devices was collected randomly as the representative setup of fluorescent images for all replicates at 0 h and at 12 h. The fluorescent image taken by an L5 filter was processed at the low scale value of 205 and the high scale value of 270, and the fluorescent image taken by a TX2 filter was processed at the low scale value of 220 and the high scale value of 290. Then the images were overlaid using MetaMorph image software (Version 6.3r1, Molecular Devices). The bright field (BF) image taken at 10 ms was processed at the low scale value of 1200 and the high scale value of 4500. The intensity profile of the fluorescent images in Fig. S2B is shown in Fig. S2C.

In Fig. S2E, fluorescein solution was used for the diffusion test of the communication channel. After a device containing deionized water in the communication channel was placed on the surface of the cover glass (24 \times 40 mm, Corning), the two culture wells were filled with deionized water using a microaspirator, and then the other culture well was filled accurately with carboxy-fluorescein solution (200 μM) under a stereomicroscope (SMZ-2E, Nikon). The device setup was inverted immediately, and fluorescent images of fluorescein diffusion were taken at 1, 5, and 15 min by an epi-fluorescence microscope (DMI 6000 B, Leica) equipped with a 5 \times objective (0.15 N.A., Leica) and an L5 filter (Leica) at 100 ms of exposure time, which

were coupled with a cooled CCD camera (12-bit, 1344 × 1024 resolution; Hamamatsu Photonics) with a 1.0× coupler. Fluorescent images were processed at the low scale value of 200 and the high scale value of 1300 by using MetaMorph image software (Molecular Devices). The BF image taken at 50 ms was processed at the low scale value of 700 and the high scale value of 4000. The intensity profile of fluorescent images in Fig. S2E is shown in Fig. S2F.

Confirmation of Chemical Gradient and Diffusion in the Microfluidic Device. In Fig. S3, the chemical gradient in the microfluidic device was demonstrated by using resorufin cellobioside (MarkerGene Fluorescent Cellulase Assay Kit, MGT Inc.), a fluorogenic substrate for the cellulases of Pc cells. Pc cells were enriched in TSB medium supplemented with 1 g/L CM-cellulose at 30°C, 180 rpm for 6 h, then washed twice with minimal buffer solution (see *SI Text*, Cultivation of Microorganisms and Culture Media), then resuspended in minimal buffer solution with a final cell density of $\approx 10^6$ CFU/ml. After the Pc cell suspension was inoculated aseptically into either one or two culture wells in a microfluidic device using the microaspirator under a stereomicroscope (SMZ-2E, Nikon), the culture wells without Pc cells were filled with minimal buffer. Then, the microfluidic device was loaded onto the surface of a cover glass (24 × 40 mm, Corning) containing resorufin cellobioside solution in the communication channel. The device setup, supported by 5-mm high polymethylsiloxane (PDMS) pieces on the cover glass (48 × 65 mm, Gold Seal), was incubated in an inverted position using the microscope incubator (Incubator BL, Pecon) at 30°C (Fig. S3A and D). Fluorescent images were taken intermittently for 3 h using an epi-fluorescence microscope (DMI 6000 B, Leica) equipped with a 5× objective (0.15 N.A., Leica) and a TX2 filter (Leica) coupled with a cooled CCD camera (12-bit, 1344 × 1024 resolution; Hamamatsu Photonics) with a 1.0× coupler (Fig. S3B and E). Red fluorescence in the culture well inoculated with Pc cells shows the fluorescence of resorufin, indicating the cleavage of resorufin cellobioside over time by Pc cells. Image acquisitions and analyses were performed as described above. After the fluorescent images in Fig. S3B and E were taken at 1, 5, 15, 60, 90, and 180 min with a TX2 filter (Leica) at 100 ms exposure time, the fluorescent images were processed at the low scale value of 210 and the high scale value of 400 by using MetaMorph image software (Molecular Devices). The intensity profile of fluorescent images in Fig. S3B and E is shown in Fig. S3C and F.

In Fig. S3G and H, the diffusion of resorufin dye was demonstrated in the microfluidic device. After Pc cells were inoculated in one of the culture wells of a device, the device was loaded onto a cover glass (24 × 40 mm, Corning) containing minimal buffer solution in the communication channel. After two culture wells without Pc cells were filled with ≈ 5 nL of minimal buffer solution, ≈ 5 nL of resorufin solution (50 μ M, 10% DMSO solution in sodium acetate buffer, MGT Inc.) was added to the culture well containing Pc cells (Fig. S3G) using a microaspirator under a stereomicroscope (SMZ-2E, Nikon). This device setup, supported by PDMS pieces 5 mm high placed on top of the cover glass (48 × 65 mm, Gold Seal), was inverted immediately and was incubated (30°C) for 30 min. Fluorescent images then were taken intermittently for 30 min using an epi-fluorescence microscope (DMI 6000 B, Leica) equipped with a 5× objective (0.15 N.A., Leica) and a TX2 filter (Leica) coupled with a cooled CCD camera (12-bit, 1344 × 1024 resolution; Hamamatsu Photonics) with a 1.0× coupler (Fig. S3H). After the fluorescent images in Fig. S3H were taken at 1, 5, 15, 20, 25, and 30 min with a TX2 filter (Leica) at 100 ms exposure time, the images were processed at the low scale value of 200 and the high scale value of 500 by using MetaMorph image

software (Molecular Devices). The intensity profile of fluorescent images in Fig. S3H is shown in Fig. S3I.

Cultivation of Three Species in a Device at High-Nutrient Medium. In Fig. S4, each species, Av, Bl, and Pc, was enriched in TSB medium (Bl and Pc) or 1771 medium (Av). After live-cell numbers of Av, Bl, and Pc species were adjusted similarly via live/dead staining (Molecular Probes), a washed cell suspension of each species was inoculated accurately into the microfluidic device using a microaspirator under a stereomicroscope (SMZ-2E, Nikon). The device containing each species in the respective culture well was loaded onto the cover glass (22 × 22 mm, Fisher Scientific), and the communication channel was filled with TSB/1771 media (4:1, vol/vol) as a high-nutrient medium. The device setup was fixed inside a Petri dish by using silicone vacuum grease (Dow Corning), and then the Petri dish containing the device setup was incubated in an inverted position at 30°C for 8 h. Water droplets were added on the bottom inside the Petri dish to maintain humidity. Three replicates of the microfluidic devices were performed in the experiment for each time point. The viability of each species in a device was confirmed by using live/dead staining (Molecular Probes). After the live/dead dye was loaded into culture wells by using the microaspirator, a cover glass (48 × 65 mm, Gold Seal) was placed over the culture wells, and the microfluidic device was inverted.

After the incubation and the live/dead staining, image acquisitions and analyses were performed in the manner described above. In Fig. S4A, fluorescent images of stained Av, Bl, and Pc species at 0 h were taken by an epi-fluorescence microscope (DMI 6000 B, Leica) equipped with a 20× objective (0.40 N.A.) and an L5 filter or a TX2 filter (Leica), at 100 ms exposure time, and coupled with a cooled CCD camera (12-bit, 1344 × 1024 resolution; Hamamatsu Photonics) with a 1.0× coupler. The reproducibility among three replicates of microfluidic devices was confirmed in all cases, and images of one of the devices were selected randomly as representative fluorescent images. The images taken with both filters were processed at the low scale value of 250 and the high scale value of 800, and the images taken with both filters then were overlaid using MetaMorph image software (Molecular Devices). In Fig. S4B, fluorescent images of stained Av, Bl, and Pc species at 8 h were taken by an epi-fluorescence microscope (DMI 6000 B, Leica) equipped with a 20× objective (0.40 N.A.) and an L5 filter or a TX2 filter (Leica) at 100 ms of exposure time. The reproducibility among three replicates of microfluidic devices was confirmed in all cases, and images of one of the devices were collected randomly as representative fluorescent images. Fluorescent images taken with both L5 and TX2 filters were processed at the low scale value of 250 and the high scale value of 1000 (Av), the low scale value of 250 and the high scale value of 4000 (Bl), and the low scale value of 250 and the high scale value of 1500 (Pc). Then, images taken with both filters were overlaid using MetaMorph image software (Molecular Devices). The intensity profiles of fluorescent images in Fig. S4A and B are shown in Fig. S4C and D, respectively.

Cultivation of a Two-Species Community in a Microfluidic Device. In Fig. S5, the stabilities of two-species and three-species communities in microfluidic devices are compared. In this figure, four experimental setups were performed simultaneously with the same seed cultures of Av, Bl, and Pc as follows: three-species community (ABC) and two-species communities (AB, AC, and BC). After seed cultures of Av, Bl, and Pc species were harvested and washed twice with minimal buffer solution (see *SI Text*, Cultivation of Microorganisms and Culture Media), the live-cell densities of each species were adjusted to a similar level of $\approx 10^6$ CFU/ml. Densities were quantified by staining with live/dead dye and then counting the cells under an epi-fluorescence microscope (DMI 6000 B, Leica). The cell suspension of each species

was transferred aseptically to sterilized Gastight syringes (1805 RN, Hamilton) with 30-gauge Teflon tubing (Weico) sealed to Teflon tubing (i.d./o.d. = 100/150 μm , PTFE, Zeus) by wax. Then, the cell suspension in the syringes was inoculated accurately into an appropriate culture well by using a microaspirator under a stereomicroscope (SMZ-2E, Nikon). In the three-species connected community, each species, Av, Bl, or Pc, was inoculated into a different culture well in a device. In the two-species connected communities, only two different species were inoculated into two different culture wells; the other culture well was left vacant. After inoculations, the device was loaded onto the surface of a siliconized glass cover slide containing CP media supplemented with 100 $\mu\text{g/L}$ glucose in the communication channel. This device setup was fixed inside a Petri dish by using silicone vacuum grease (Dow Corning), then water droplets were added on the bottom of the inside of the Petri dish for maintaining humidity, and finally the Petri dish containing the device setup was incubated in an inverted position at 30 °C. Three replicates of microfluidic devices were performed for every experiment at each time point. After the incubation, image acquisitions and analyses were performed in the same way as described above. Normalized live cell numbers were obtained by dividing the live numbers of each species at each time point by those numbers at 0 h.

Full Mathematical Model Including Colony Growth. In Fig. 4, mathematical analysis of a model community was used to explain how spatial structure influences the coupling of microbial communities. In that model it was assumed that colony size did not change over time. Below is a full model that includes terms for the growth of colonies. The full model demonstrates that the model system has a global steady state (colony sizes and nutrient concentrations are simultaneously stable and non-zero) only for a range of intermediate distances.

To analyze the stability of the model in Fig. 4 to separation distance (L), concentration of A ($[A]_\alpha$), concentration of B ($[B]_\beta$), size of colony alpha (N_α) and size of colony beta (N_β), a logistic growth equation for colonies α and β was used:

$$\frac{\partial N_\alpha}{\partial t} = \mu_\alpha \times N_\alpha \times (1 - N_\alpha/K_\alpha) \quad (1)$$

$$\frac{\partial N_\beta}{\partial t} = \mu_\beta \times N_\beta \times (1 - N_\beta/K_\beta) \quad (2)$$

K_χ is the carrying capacity for colony χ . In the model system, carrying capacity is a function of nutrients A and B, therefore we modeled the carrying capacity as:

$$K_\alpha = \frac{k_\alpha \times [A]_\alpha \times [B]_\alpha(L)}{(k_{\alpha,A} + [A]_\alpha) \times (k_{\alpha,B} + [B]_\alpha(L))} \quad (3)$$

$$K_\beta = \frac{k_\beta \times [A]_\beta(L) \times [B]_\beta}{(k_{\beta,A} + [A]_\beta(L)) \times (k_{\beta,B} + [B]_\beta)} \quad (4)$$

Equations for the change over time of $[A]_\alpha$ and $[B]_\beta$ are:

$$\begin{aligned} \frac{\partial [A]_\alpha}{\partial t} = & \frac{k_1 \times [A]_\alpha^3 \times ([B]_\alpha(L))^3}{(k_2 + [A]_\alpha^3) \times (k_3 + ([B]_\alpha(L))^3)} \times N_\alpha - k_4 \times [A]_\alpha \times N_\alpha \\ & - k_9 \times [A]_\beta(L) \times N_\beta \end{aligned} \quad (5)$$

$$\begin{aligned} \frac{\partial [B]_\beta}{\partial t} = & \frac{k_5 \times ([A]_\beta(L))^3 \times [B]_\beta^3}{(k_6 + ([A]_\beta(L))^3) \times (k_7 + [B]_\beta^3)} \times N_\beta - k_8 \times [B]_\beta(L) \\ & \times N_\alpha - k_{10} \times [B]_\beta \times N_\beta \end{aligned} \quad (6)$$

For this analysis, the variable d was used to simplify the terms $[A]_\beta(L)$ to $[A]_\alpha \times (1-d)$ and $[B]_\alpha(L)$ to $[B]_\beta \times (1-d)$. The value of d is between 0 and 1, and d is a function of the transport properties of the system. For example, $(1-d)$ represents the fraction of nutrient A at colony α that arrived at colony β . When $d = 1$, the separation distance is infinite, and colony β receives no nutrient A. When $d = 0$, the separation distance is 0, and both colony α and colony β receive the same amount of nutrient A.

It should be noted that the Damköhler number (D_a) should be large for spatial effects to be important in coupled systems such as the two-species model used in Fig. 4. The Damköhler number is a dimensionless parameter that defines the relative rates of transport and reaction. If D_a is large, spatial gradients of released products will form, and therefore the coupling of the system will be a function of space. In our system, we defined the D_a as $(L^2 \times k_{\text{consumption}})/D$, where L is the separation distance (m), $k_{\text{consumption}}$ is the consumption rate (s^{-1}), and D is the diffusion constant (m^2s^{-1}). Based on experimentally measured values, we predicted that the community and devices used in the experiments should be in the regime in which released products form a gradient, as observed in Fig. S3.

These equations give rise to communities of Class I, II, or III as described in the main text. The class of a given community depends on the values of the rate constants in the equations in a manner consistent with the metabolic analysis presented in the main text. To illustrate the stability of a Class II community to perturbations in concentrations, populations, and distance, we chose at random values of the rate constants (listed in Table S1) which corresponded to a Class II community. To analyze the stability of these steady states, we used Equations 1-6 to evolve the system over time at different values of d to examine the stability of $[A]_\alpha$, $[B]_\beta$, N_α , and N_β . Mathematica (Mathematic 6.0, Wolfram Research Inc.) was used for these simulations, with initial conditions of $[A]_\alpha = 6.5$, $[B]_\beta = 3.0$, $N_\alpha = 0.35$ and $N_\beta = 0.13$, which are near a global steady state of the system.

As shown in Fig. S6, the system was able to establish a steady state for any distance 0.21 [lteq] d [lteq] 0.72. If the colonies were separated by intermediate distances and given suitable initial conditions, the system was able to establish a global steady state, indicating that the model system is Class II.

Next, the stability of the global steady state to fluctuations of each variable was demonstrated. The system with $d = 0.5$ was perturbed every 250 time points starting at time point 250. The perturbation consisted of changing the value of one of the variables by $\pm 20\%$ (as indicated in Fig. S7 A-D). All system variables returned to the steady-state value after each perturbation, indicating that the system has a non-zero steady state that is stable.

The global steady state of the system was determined over the range of d . The initial conditions of the system were $[A]_\alpha = 6.5$, $[B]_\beta = 3.0$, $N_\alpha = 0.35$, and $N_\beta = 0.13$, which are near a global steady state. The steady state was calculated for d between 0 and 0.95 in increments of 0.01 by simulating 50,000 time steps for each d value. Values of d near 1 experienced numerical errors because of dividing by numbers near zero. The results of the simulation are shown in Fig. S7 E-H. The system was not stable at close distances (low values of d), because the steady state is zero for all variables. At intermediate distances, non-zero steady states were reached. As d increases in the intermediate regime, steady-state concentrations of $[A]_\alpha$ and $[B]_\beta$ increased because of decreased nutrient competition as predicted by the model in Fig. 4. At large values of d (i.e., when the colonies were far apart), the steady states again evolved to zero for all variables.

Analysis of the full model which includes growth terms for colonies α and β was in agreement with the simplified analysis presented in main text. The full model demonstrated that including growth terms for the colonies did not destabilize a Class II community. In addition, the full model was used to

calculate the range of d over which the community has non-zero steady states.

Measurements of Cellulase Activity. In Fig. S8, the enzymatic activity of cellulase was measured by using the fluorogenic substrate 4-methylumbelliferyl β -D-cellobioside (4-MUFC, Sigma-Aldrich). To measure the cellulase activity of Pc cells at different concentrations of glucose, Pc cells enriched in TSB medium were washed twice and resuspended in the incubation media containing different concentrations of glucose (0, 0.01, 0.03, 0.1, 0.3, 0.6, 1, 2.5, 5, 7.5, 10, 25, 50, and 100 μ M) and a corresponding concentration of casamino acid in the minimal buffer solution (see *SI Text*, Cultivation of Microorganisms and Culture Media) at 30°C for 6 h. In these incubation media, the carbon/nitrogen (C/N) ratio of glucose to casamino acid was held constant at 10 (wt/wt). During the 6-h preincubation, fresh incubation medium supplemented with glucose and casamino acid was supplied to the culture by spinning down the cells, removing old medium, and adding fresh medium every 2 h. After 6 h, carboxymethyl-cellulose (1 g/L, final concentration) was added to the minimal buffer/glucose/casamino acid solution, and the cell suspension then was incubated for 2 h to induce cellulase activity. Next, this cell suspension was concentrated to a 1/10 volume ratio and was used to measure cellulase activity. After 50 μ l of the Pc cell suspension was mixed with 50 μ l of the 4-MUFC solution (500 μ M) in a sterilized 96-well plate (Costar 3603, Corning Inc.), the plate was incubated at 30°C for 1 h. Then, 100 μ l of glycine buffer (0.2 M, pH 10.0) was added, and the fluorescence intensity ($\lambda_{\text{ex}}/\lambda_{\text{em}} = 365/455$ nm) of 4-methylumbelliferone (4-MUF), a cleaved product, was measured immediately using a microplate reader (Safire², Tecan Group Ltd). A calibration curve was obtained for 4-MUF (Sigma-Aldrich), and this curve was used to estimate the concentration of products cleaved from 4-MUFC by Pc cells.

Measurements of Glucose Concentration. In Fig. S8, glucose concentrations were measured by using enzymatic reactions of glucose oxidase (Amplex red glucose/glucose oxidase assay kit, Molecular Probes, Invitrogen). Av and Pc cells were enriched in 1771 and TSB media, respectively, were washed twice with minimal buffer solution (see *SI Text*, Cultivation of Microorganisms and Culture Media), and then were resuspended at 10^6 cfu/ml in 14-ml test tubes (Falcon, Becton Dickinson Labware) with a 5-ml working volume of incubation medium. The incu-

bation media contained various concentrations of glucose (0, 1, 5, 10, 50, and 100 μ M) and corresponding levels of casamino acid (Acros) in the minimal buffer solution. The C/N ratio of glucose to casamino acid was held constant at 10 (wt/wt). Both Av and Pc cells were preincubated in incubation media with different levels of glucose and casamino acid for 6 h. During the 6-h preincubation, fresh incubation medium supplemented with glucose and casamino acid was supplied to the culture by spinning down the Av or Pc cells, removing old medium, and adding fresh incubation medium every 2 h. After preincubation, old incubation media were replaced with the fresh incubation media containing different levels of glucose and casamino acid in the minimal buffer solution, and cells then were reincubated for 3 h. Samples of 1 ml were taken every 1 h and used for measuring optical density at 600 nm (8453 UV-Visible Spectrophotometer, Agilent Technologies). Immediately after cells were removed from the sample solution by filtration (0.45 μ m, Whatman), the culture filtrate was stored in a deep freezer at -70°C until the enzymatic assay was performed. To perform the assay, samples were thawed by incubating at room temperature for 30 min. Next, an aliquot was mixed with an equal volume of glucose oxidase reagent containing Amplex Red reagent (10-acetyl-3,7-dihydroxyphenoxazine), horseradish peroxidase, and glucose oxidase in a sterilized 96-well plate (Costar 3603, Corning Inc.). The plate then was incubated at 30°C for 30 min. The glucose concentration was estimated by the fluorescence intensity ($\lambda_{\text{ex}}/\lambda_{\text{em}} = 571/585$ nm) of resorufin, a reaction product, using a microplate reader (Safire², Tecan Group Ltd). The calibration curve was obtained for various concentrations of glucose solution, and the curve then was used to estimate glucose concentration in the culture broth.

Acquisition of Fluorescence Intensity of Fluorescent Images. The intensity profile of fluorescent images was obtained from line scans of each fluorescent image by using MetaMorph image software (Molecular Devices). In the overlaid fluorescent images taken by an L5 filter and a TX2 filter, the fluorescence intensity was obtained from each image, and then the intensity profile was plotted in the same graph. The width of the line scan was set to 10 pixels in all cases. The dark current of the camera was subtracted from all fluorescent images. The dark current was obtained by taking images without any specimen on the stage in an epi-fluorescence microscope (DMI 6000 B) using either an L5 filter or a TX2 filter (Leica). The dark current was 201 for both filters.

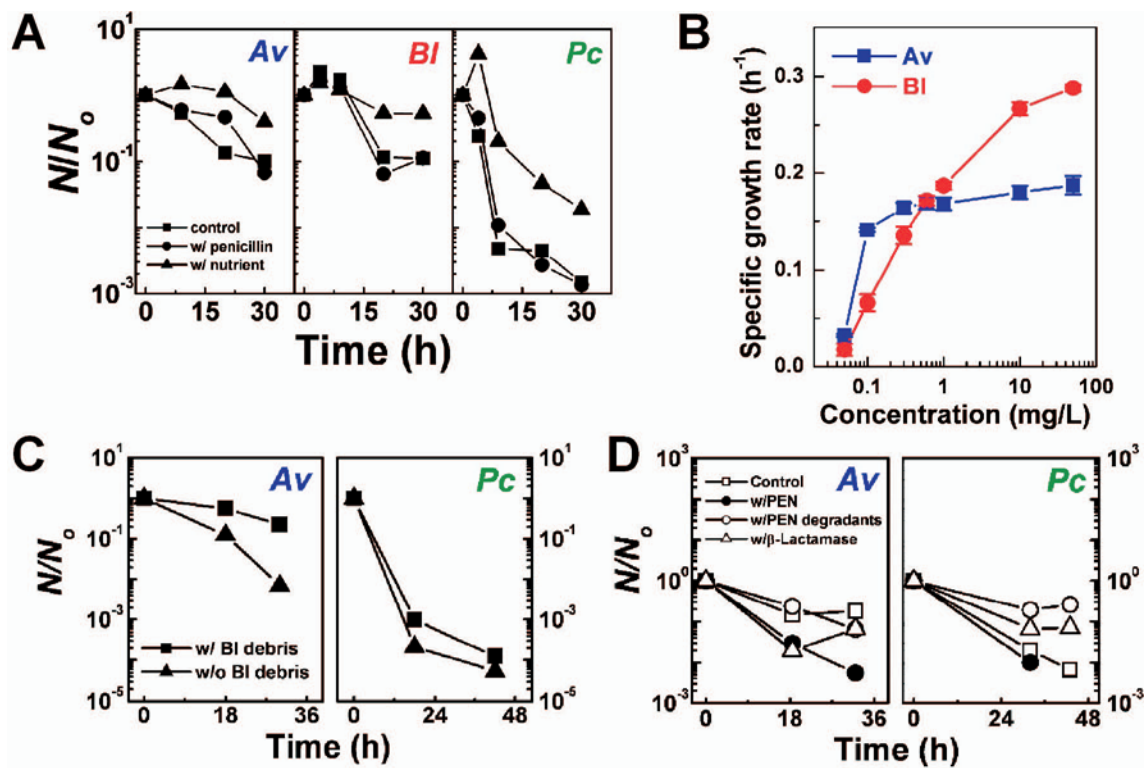


Fig. S1. (A) The survival ratio of each species decreased over time when each species was incubated in a pure culture in a test tube under stressful conditions. The survival ratio was defined as the normalized number of viable cells at each time point divided by the number of viable cells at 0 h. Graphs show the survival ratio (N/N_0) of each species over time when cultured in isolation in a no-nutrient medium (black squares; control; minimal buffer, see *SI Text*), in a no-nutrient medium with antibiotics (black circles; w/penicillin; minimal buffer supplemented with 100 mg/L penicillin G), and in a low-nutrient medium (black triangles; with nutrient; minimal buffer supplemented with 500 μ M glucose and 500 μ M ammonium phosphate). The survival ratio of each species decreased over time in all media conditions. (B) Specific growth rates of either Av (blue squares) or Bt (red circles) species in pure cultures at different nutrient levels. Graphs show that Bt cells have higher growth rates than Av cells in high-nutrient conditions (1 mg/L of TSB/1771 medium), whereas Av cells have higher growth rates than Bt in very low-nutrient conditions (<0.5 mg/L of TSB/1771 medium). The TSB/1771 medium (4:1, vol/vol) was diluted from the initial concentration of TSB medium (30 g/L). Concentrations of the medium reported on the x-axis were calculated from the extent of dilution (e.g., a 30,000-fold dilution corresponds to a concentration of 1 mg/L on the x-axis). Error bars indicate standard error. (C) The effect of heat-killed Bt debris on the viable cell numbers of either Av or Pc cells cultured individually over time. Graphs show that the survival ratio (N/N_0) of Av (Left) and Pc (Right) decreased over time in the presence (with Bt debris, solid squares) or the absence (without Bt debris, solid triangles) of heat-killed Bt debris (see *SI Text*, Effect of Heat-Killed Bt Cell Debris on the Viability of Av and Pc Cells). The survival ratio was obtained by dividing the number of viable cells per well at each time point by the number of viable cells per well at 0 h. The number of viable cells of each species was obtained by using the plate-counting method. (D) The effect of degradation products of penicillin G on the viability of either Av or Pc cells. Graphs show the survival ratio (N/N_0) of Av (Left) and Pc (Right) over time. The control medium (open squares) consisted of the minimal buffer with 1 g/L CM-cellulose and 100 μ g/L glucose. Other media consisted of control medium supplemented with 100 mg/L penicillin G (w/PEN; solid circles), with the degradation products of penicillin G by the β -lactamase (w/PEN degradants; open circles), or with 0.5 mg/L β -lactamase (w/ β -Lactamase; open triangles). Results indicate that viability of either Av or Pc over time is not affected greatly by the presence of degradation products of penicillin G (see *SI Text*, Effect of Penicillin and Its Degradation Products on the Viability of Av and Pc Cells). The survival ratio was obtained by dividing the number of viable cells per well at each time point by the number of viable cells per well at 0 h. The number of viable cells of each species was obtained by using the plate-counting method. The degradation of penicillin G by β -lactamase was confirmed by thin-layer chromatography (data not shown).

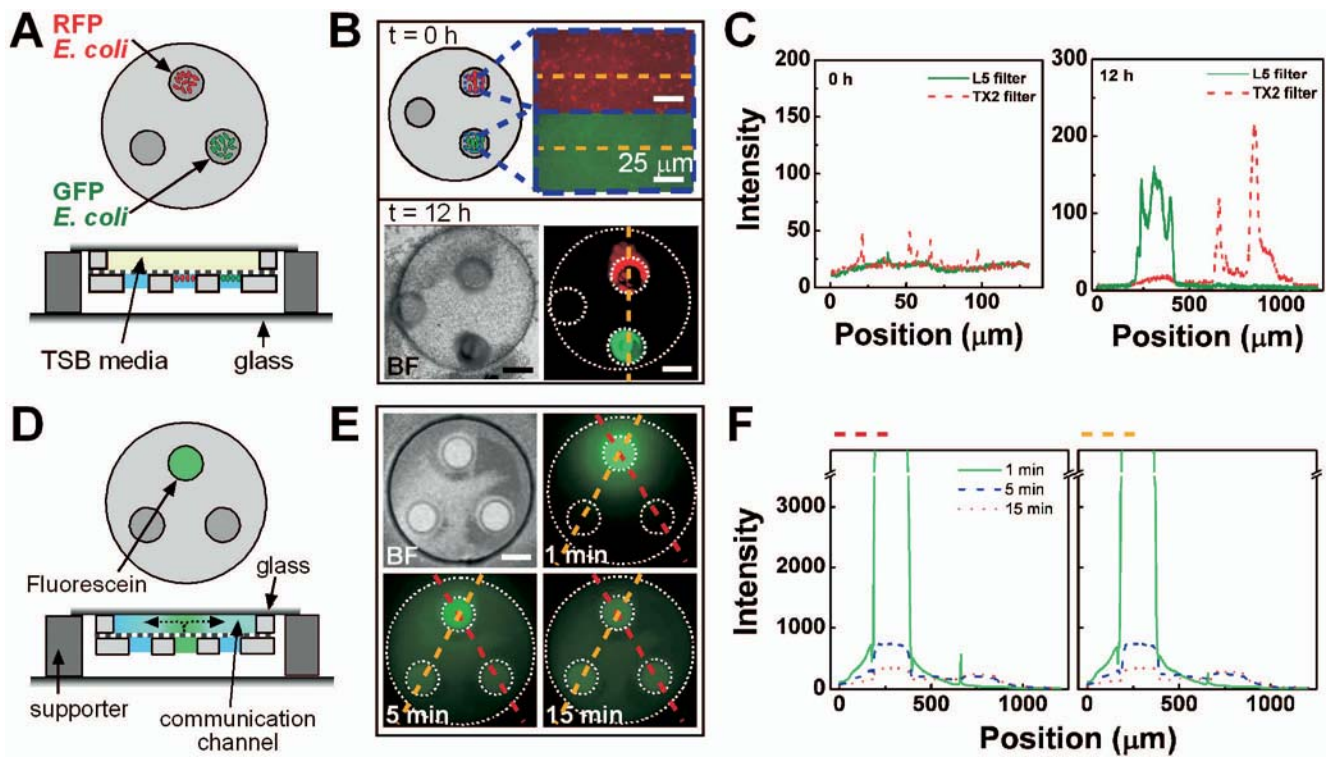


Fig. S2. Confirmation of the localized growth of species in spatially segregated culture wells over time and the maintenance of chemical communication in the microfluidic device (see *SI Text*, Confirmation of Localized Growth of Bacterial Species in the Microfluidic Culture Well). (A) A schematic drawing describes the experimental setup in the microfluidic device. (B) A BF image of the device and a fluorescence image showed the localized growth of different *E. coli* strains expressing either green or red fluorescent proteins in spatially segregated culture wells without cross-contaminations. Orange dashed lines indicate the scanned position in the fluorescence image. Scale bars indicate 200 μm . (C) Intensity profiles of fluorescent images in Fig. S2B. In the intensity profile, "L5 filter" indicates the intensity profile of fluorescent images for the GFP-labeled *E. coli* strain taken by the L5 filter, and "TX2 filter" indicates the intensity profile of fluorescent images for the RFP-labeled *E. coli* strain taken by the TX2 filter (see *SI Text*, Acquisition of Fluorescence Intensity of Fluorescent Images). (D) A schematic drawing describes the experimental setup in the microfluidic device. (E) A BF image of the device and fluorescence images showed diffusion of fluorescein through the communication channel, confirming connectivity between wells. Red and orange dashed lines indicate the scanned position in the fluorescent image, respectively. Scale bars indicate 200 μm . (F) Intensity profiles of fluorescent images in Fig. S2E. The intensity profile was obtained from fluorescent images taken by the L5 filter.

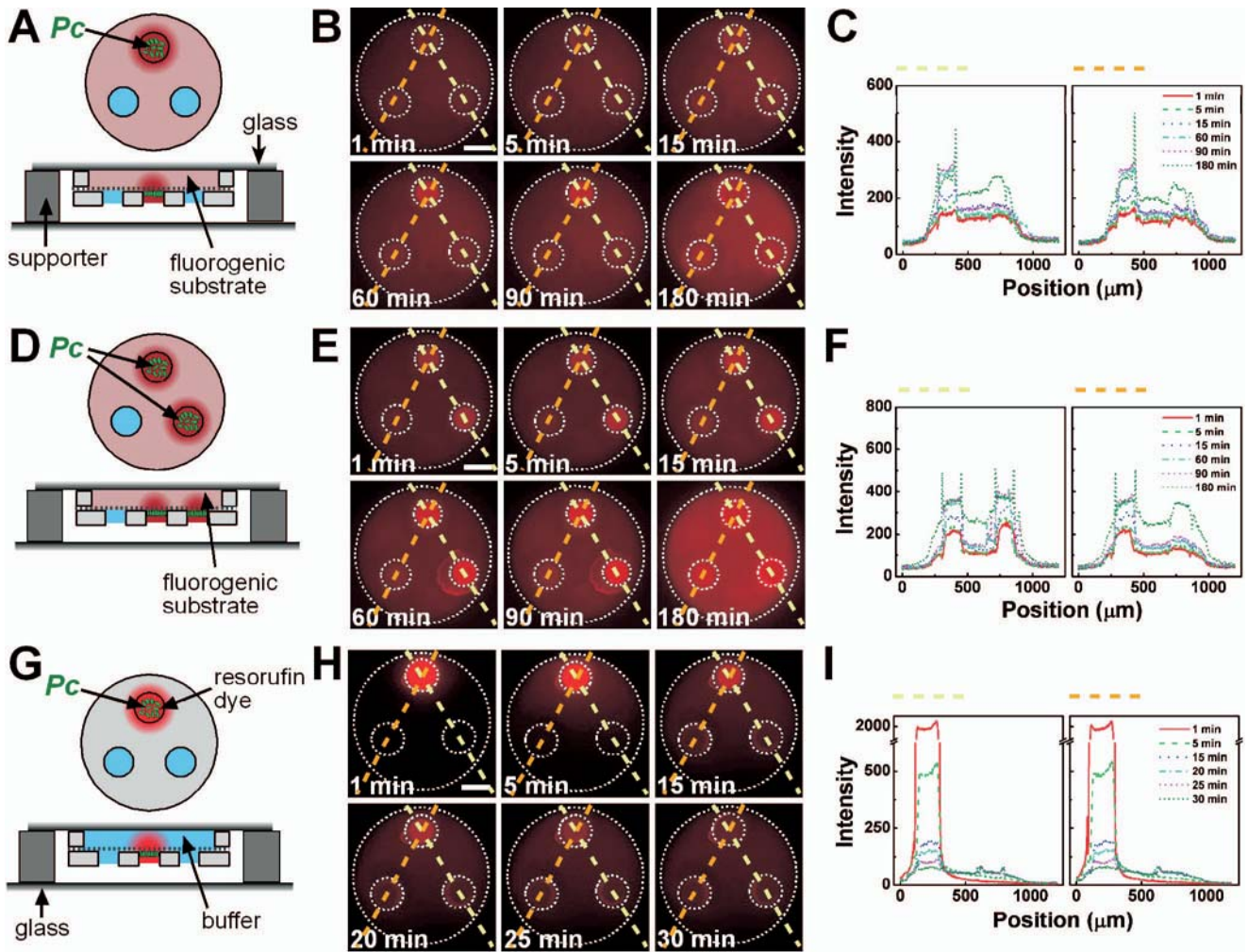


Fig. S3. Confirmation of chemical gradient and diffusion of fluorescent molecules over time in the microfluidic device (see *SI Text*, Confirmation of Chemical Gradient and Diffusion in the Microfluidic Device). (A) A schematic drawing of the experimental setup in the microfluidic device. (B) The fluorescent images of the cleaved product (resorufin) from the degradation of fluorescence-labeled resorufin cellobioside by Pc cells inoculated in a single spatially segregated culture well. (C) Intensity profiles of fluorescent images in Fig. S3B. (D) A schematic drawing of the experimental setup in the microfluidic device. (E) The fluorescent images of the cleaved product (resorufin) from the degradation of fluorescence-labeled resorufin cellobioside by Pc cells inoculated in two spatially segregated culture wells. (F) Intensity profiles of fluorescent images in Fig. S3E. (G) A schematic drawing of the experimental setup in the microfluidic device. (H) The fluorescent images of diffusion of resorufin dye (50 μ M) through the communication channel. (I) Intensity profiles of fluorescent images in Fig. S3H. The intensity profiles were obtained from fluorescent images taken by the TX2 filter (see *SI Text*, Acquisition of Fluorescence Intensity of Fluorescent Images). Yellow and orange dashed lines in B, E, and H indicate the scanned position in each fluorescent image.

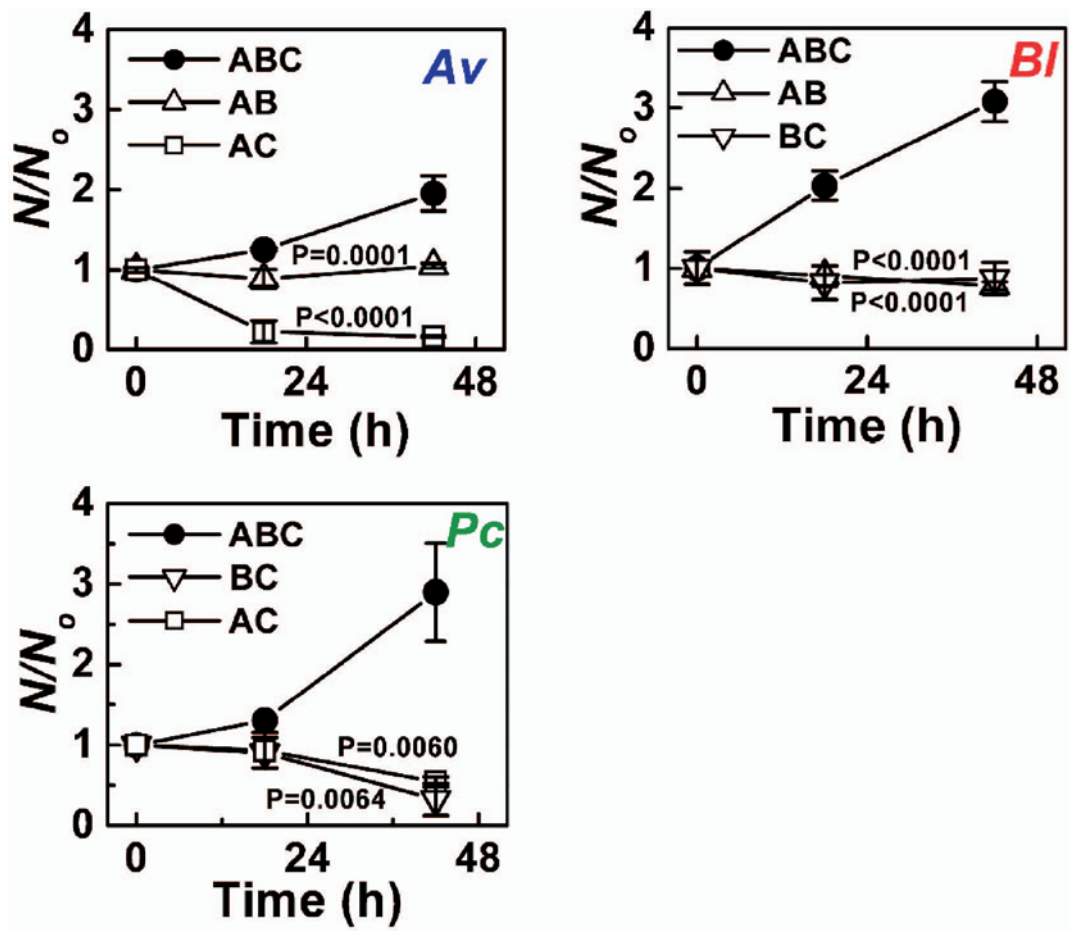


Fig. 55. Comparison of survival ratio (N/N_0) in the communities cultured in a device with three species (ABC) versus communities cultured in a device with two species (AB, BC, or AC). A is Av, B is BI, and C is Pc. Each species showed the highest number of cells when cultured in a connected community with three species, compared with two-species connected communities. Graphs show the survival ratio as a function of time; each species was cultured in an individual, connected well of the microfluidic device in CP medium at 30°C. The survival ratio was obtained by dividing the number of live cells per well at each time point by the number of live cells per well at 0 h. Error bars indicate standard errors. P-values were calculated using two-way ANOVA by comparing the three-species community with each two-species community.

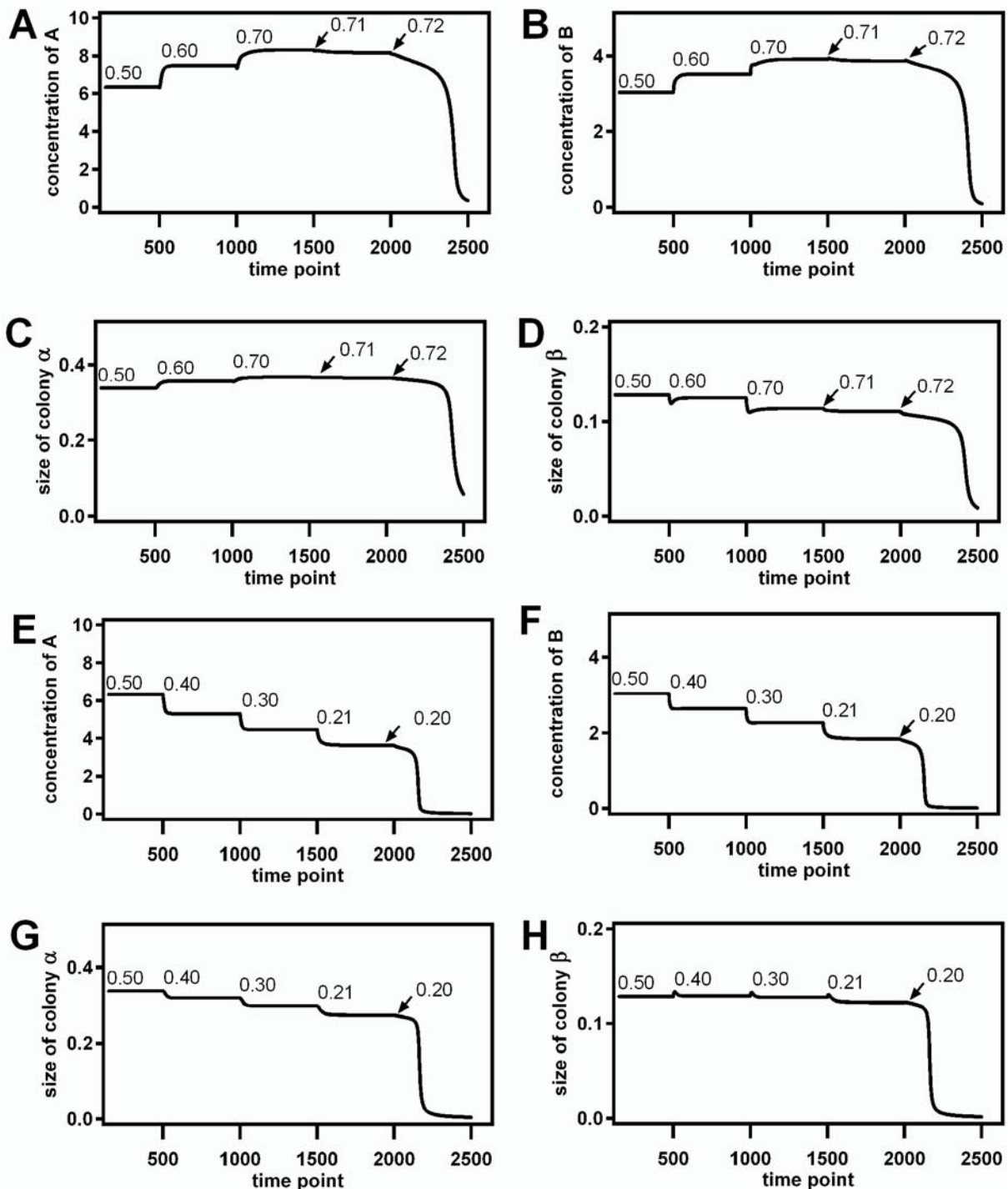


Fig. S6. Responses of parameters in the two-colony model to increasing and decreasing d . Parameter d is a descriptor of the separation distance between colonies α and β . The value of d was increased (A–D) or decreased (E–H) every 500 time points. For perturbations up to time point 2000, the system reestablished steady-state levels of $[A]_{\alpha}$, $[B]_{\beta}$, N_{α} , and N_{β} for both increasing and decreasing d . For both cases, at time point 2000 a perturbation was made that evolved the system toward zero concentrations of all variables. Numbers above the curves indicate values of d . Graphs start at time point 150; at that point the system had established a steady state. (A) Response of concentration of A. (B) Response of concentration of B. (C) Response of size of colony α . (D) Response of size of colony β . (E) Response of concentration of A. (F) Response of concentration of B. (G) Response of size of colony α . (H) Response of size of colony β .

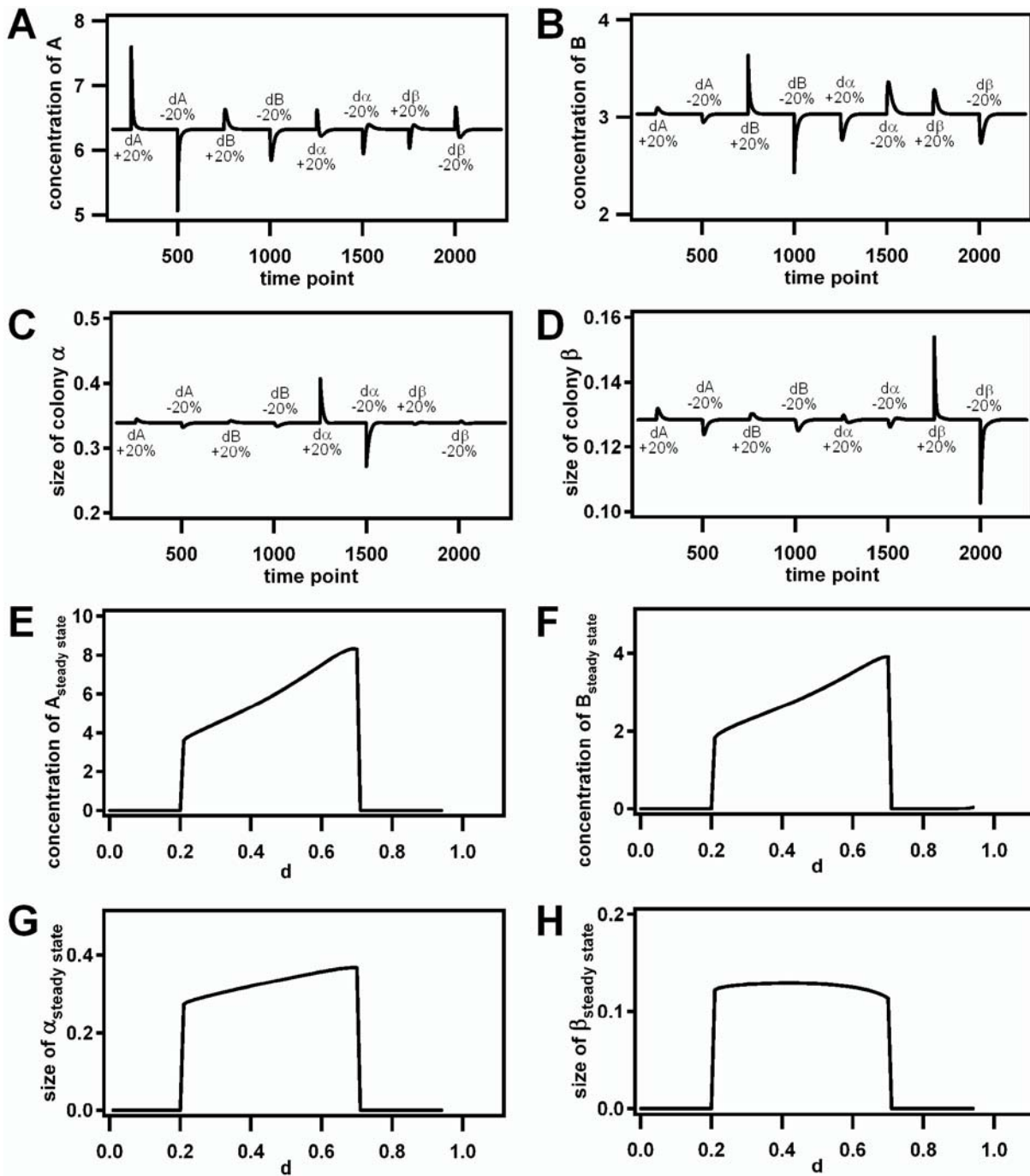


Fig. S7. Stability analysis of parameters of the two-colony model system at $d = 0.5$ and steady-state values of parameters as a function of d . Parameter d is a descriptor of the separation distance between colonies α and β . (A–D) Every 250 time points, a different variable was perturbed by $\pm 20\%$ of the steady-state value, as indicated on each curve. Each variable returned to the initial steady state after each perturbation, indicating that the system has a global steady state that is stable. (A) Response of concentration of A. (B) Response of concentration of B. (C) Response of size of colony α . (D) Response of size of colony β . (E–H) Steady state values were simulated for d between 0 and 0.95 in increments of 0.01. The system has a global steady state for intermediate values of d , indicating that the model system is a Class II community. Graphs start at time point 150; at that point the system had established a steady state. (E) $[A]_{\text{steady state}}$. (F) $[B]_{\text{steady state}}$. (G) N_{α} . (H) N_{β} .

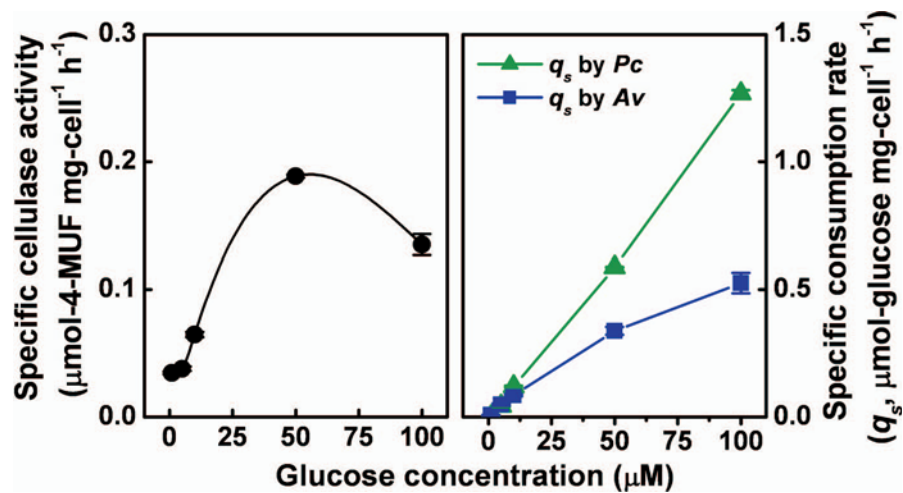


Fig. 58. Profiles of specific cellulase activity by Pc cells (*Left*) and of specific consumption rate (q_s) of glucose (*Right*) by either Av or Pc cells as a function of glucose concentration. Graphs show a profile of a nonlinear production rate by Pc cells (*Left*) and linear consumption rates of glucose by Av and Pc cells (*Right*). The specific cellulase activity, as approximated by the cleavage rate of the fluorogenic substrate 4-MUFC by Pc cellulases, was a nonlinear function of glucose concentration. To obtain the specific cellulase activity as the function of glucose concentrations, Pc cells were preincubated in minimal buffer over 6 h with different levels of glucose and corresponding levels of casamino acid, followed by CM-cellulose induction for 2 h (see *SI Text*, Measurements of Cellulase Activity). Specific cellulase activity then was obtained by the calibration curve from 4-MUF. To obtain the specific consumption rate of glucose as the function of glucose concentrations, both Av and Pc cells were preincubated in minimal buffer for 6 h with different levels of glucose (0, 1, 5, 10, 50, and 100 μM) and corresponding levels of casamino acid, then were reincubated in minimal buffer solution supplemented with various concentrations of glucose and corresponding levels of casamino acid (see *SI Text*, Measurements of Glucose Concentration). The specific consumption rate of glucose then was calculated by the enzymatic assay using glucose oxidase. Error bars indicate standard error.

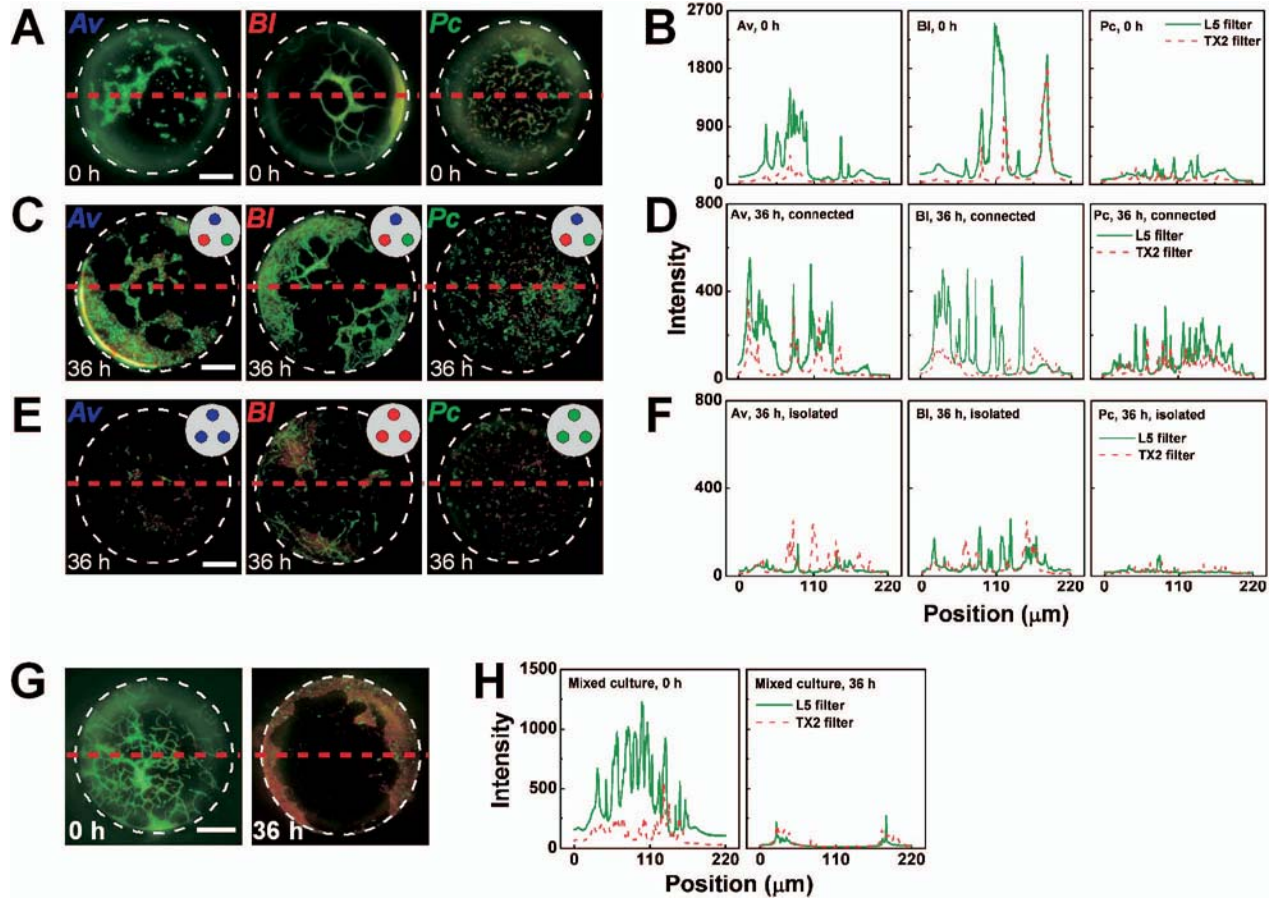


Fig. S9. Intensity profiles of fluorescent images in Fig. 2 *A* and *B* in the main text. (*A*) Images from Fig. 2 *A* in the main text at 0 h were used for the line scan. (*B*) Intensity profiles of fluorescent images in Fig. S9*A*. (*C*) Images from Fig. 2 *A* in the main text at 36 h were used for the line scan. (*D*) Intensity profiles of fluorescent images in Fig. S9*C*. (*E*) Images from Fig. 2 *B* in the main text were used for the line scan. (*F*) Intensity profiles of fluorescent images in Fig. S9*E*. (*G*) Images from Fig. 3*A* in the main text were used for the line scan. (*H*) Intensity profiles of fluorescent images in Fig. S9*G*. In all fluorescent images, red dashed lines indicate the scanned position in the image. In all intensity profiles, "L5 filter" indicates the intensity profile of fluorescent images taken by the L5 filter, and "TX2 filter" indicates the intensity profile of fluorescent images taken by the TX2 filter (see *SI Text*, Acquisition of Fluorescence Intensity of Fluorescent Images).

